# Advanced manufacturing of microscale light-emitting diodes and their use in displays and biomedicine

## Junyu Chen, He Ding & Xing Sheng

Published online: 04 Sep 2023.

Submit your article to this journal ⤤

Article views: 681

View related articles ⤤

View Crossmark data ⤤

Citing articles: 1 View citing articles ⤤

**Taylor & Francis**
Taylor & Francis Group

# Advanced manufacturing of microscale light-emitting diodes and their use in displays and biomedicine

Junyu Chen [a], He Ding [b] and Xing Sheng [a]

aDepartment of Electronic Engineering, Beijing National Research Center for Information Science and Technology, Center for Flexible Electronics Technology, and IDG/McGovern Institute for Brain Research, Tsinghua University, Beijing, People's Republic of China; bBeijing Engineering Research Center for Mixed Reality and Advanced Display, School of Optics and Photonics, Beijing Institute of Technology, Beijing, People's Republic of China

**ABSTRACT**

Thin-film, microscale light-emitting diodes (micro-LEDs)-based III–V compound semiconductors are emerging as a promising technology for next-generation light sources with various applications including lighting, display and biomedicine. With this perspective, we provide an overview and highlight our own progress on the recent developments in advanced manufacturing techniques and potential applications of micro-LEDs. The combination of epitaxial lift-off and transfer printing techniques have produced ultraminiaturized, highly luminous, and energy-efficient thin-film micro-LEDs, with a wide range of applications. To achieve full-color displays, several approaches have been developed, including horizontally and vertically assembled red-green–blue (RGB) pixels, and quantum dot conversion. For neuroscience studies, these micro-LEDs can be integrated in flexible probes as implantable light sources, which facilitate light delivery into the deep brain tissue for optogenetic stimulations and biological sensing. Additionally, micro-LEDs have the potential to function as wireless biosensors to detect changes in the biological environment, through their luminescence or in combination with other devices. Overall, advanced manufacturing techniques produce micro-LEDs that promise significant applications not only in displays but also in various biomedical fields.

## 1. Introduction

The discovery of electroluminescence on silicon carbide (SiC) by Henry Joseph Round in 1907 marked the beginning of light-emitting diodes (LEDs) technology, which attracted enormous interest and progressed tremendously in the past century [1]. Gallium arsenide (GaAs)-based infrared LEDs, gallium phosphide (GaP)-based red LEDs, and gallium nitride (GaN)-based blue LEDs were successively developed in the 1960s and 1990s, playing important roles in the growth of the modern lighting and display industry [2–5]. Unlike incandescent bulbs based on a heated filament and fluorescent bulbs based on phosphorescent coating absorbing ultraviolet light from electrically activated gases, LEDs produce light by directly injecting electric currents through semiconductor devices, providing energy-efficient and long-lasting lighting and disruptive lighting. Nowadays, LED-based displays exhibit performance superior to other technologies, such as liquid crystal displays (LCDs), organic LEDs (OLEDs), quantum dot, and perovskite-based LEDs, in terms of their efficiency, brightness, contrast, dynamic

response, and long-term stability [6–8]. Furthermore, the growing demand for high-resolution and high-gamut displays has been driven by a wide range of applications, including entertainment, medical imaging and professional work [9, 10]. Thin-film microscale LEDs (micro-LEDs) with lateral dimensions less than 100 $\mu$m, and featuring high brightness, small footprints, low power consumption and long lifespan have emerged as a promising candidate and provide a route to next-generation displays and biomedical light sources [8, 11].

Reducing the size of LEDs comes with benefits such as improved display resolution and lower raw material costs, but it also presents notable difficulties in terms of drastic decrease in efficiency, deteriorated uniformity alignment, and positioning. The first monochromatic micro-LED display was developed using III-nitride blue Micro-LEDs, consisting of an array of $10 \times 10$ pixels with a single diameter of 12 µm [12, 13]. Since then, researchers have further proposed full-color micro-LED displays using color conversion represented by quantum dots or red, green, and blue (RGB) micro-LED combinations, and

---

pilot products have been launched in the display industry [8]. As these advancements in micro-LED technology greatly improve visual quality and realism, virtual reality (VR) and augmented reality (AR) devices are more controllable to achieve stunning visual effects [14, 15]. Micro-LEDs also play a role in Li-Fi systems in the field of communication [16–18]. In addition to applications in information display, III-V micro-LEDs have led to a range of exciting new applications in various other fields, especially the biomedicine field. For example, these micro-LEDs can be used as implantable light sources for neuro photostimulation in the biological field [19–21], incorporated into tiny biosensors to measure physiological signals such as electrical activity, temperature, and pressure [22–25], etc. In this perspective, we start by introducing techniques to produce thin-film micro-LEDs, and then highlight their recent (including our own) demonstrations in the areas of advanced display light sources for biological stimulations, and wireless biosensors.

## 2. Fabrication of micro-LEDs: epitaxial lift-off and transfer printing

The development of micro-LEDs presents several technical challenges, particularly in relation to production processes, efficiency, and color tunability. To address these challenges, various approaches have been explored, including wafer-scale transfer, surface roughening, and the integration of multiple colors [8, 26–28]. Fabricating thin-film micro-LEDs using epitaxial lift-off and transfer printing can be an appealing choice among these methods. First, thin-film LEDs can be combined with substrates through transfer printing, ensuring high throughput for mass production [29, 30]. Second, the micro-LEDs can be fabricated in extremely thin layers by various deposition technologies allowing for fantastic flexibility in design and fabrication, which means multilayer stacking becomes possible [31–33]. Furthermore, the utilization of traditional LED growth techniques in the fabrication of micro-LEDs yields exceptional optoelectronic performance. Transfer technology provides a way to retain and utilize these remarkable characteristics in integrated circuits or other applications, thereby enabling micro-LEDs to combine the benefits of traditional LED performance. Consequently, transfer technology expands the potential applications of micro-LEDs in various fields.

The production of thin-film micro-LEDs involves several essential steps, including epitaxial structure growth, microscale device fabrication, release from the source wafer, and transfer printing onto the target substrate or circuit. However, the release process for GaAs-based and GaN-based micro-LEDs differs due to the utilization of distinct growth substrates [27, 29, 33, 34]. Sacrificial layer wet etching is a widely used method for the production of red, yellow, and infrared GaAs-based LEDs. Alternatively, laser lift-off, a special epitaxial lift-off method using a laser to selectively delaminate and transfer nitride layers, is typically employed for GaN-based blue, green, and violet LEDs [35]. Figure 1a provides a schematic representation of the fabrication and transfer printing process utilized for red, yellow, and infrared LEDs, which are commonly grown on GaAs substrates [33]. The sacrificial layer is selectively removed in an etching solution and is commonly utilized for the production of red, yellow, and infrared LEDs. For instance, hydrofluoric acid (HF) is employed to etch the sacrificial AlAs layer that is inserted between the LED structure and the GaAs substrate. To prevent the LEDs from detaching during the etching process, patterned photoresist is applied on the corners around the device to serve as a tether that links the LEDs to the substrate. Subsequently, an elastomeric stamp made of patterned PDMS is used to attach the micro-LEDs via Van der Waals force and then swiftly peel them away from the source wafer. The stamp is then aligned with the devices on the target substrate and pressed onto the heterogeneous substrate. By adjusting the stamp speed, the adhesion force between the device and the stamp can be modified, subsequently facilitating the transfer printing of the devices onto a heterogeneous substrate. Figure 1b depicts a schematic illustration of the fabrication and transfer printing process employed for blue, green, and violet LEDs, which are typically grown on a sapphire substrate with a GaN buffer layer. Laser lift-off is used to decompose the GaN buffer layer, leading to the formation of gallium metal and nitrogen gas. Due to the laser shock, a thermal release tape is used to fix the release devices instead of the photoresist. The micro-LEDs are then detached from the sapphire substrate by applying mild mechanical force at 70°C (above the melting point of gallium, which is approximately 29.7°C). The residual gallium is then removed by immersing the samples into a dilute ammonia solution (1:5 in water) at room temperature for approximately 30 min. Following this step, the thin-film micro-LEDs are detached from the temporary release tape (TRT) by heating them to 120°C, since the critical release temperature is roughly 110°C. This process enables the GaN-based micro-LEDs to be transferred onto a heterogeneous substrate using polydimethylsiloxane (PDMS).

Figure 1c showcases a series of microscope images exhibiting different micro-LEDs that have been transferred onto glass substrates, with and without electroluminescence. As shown in Figure 1d, these transferred devices emit light with wavelengths ranging from blue
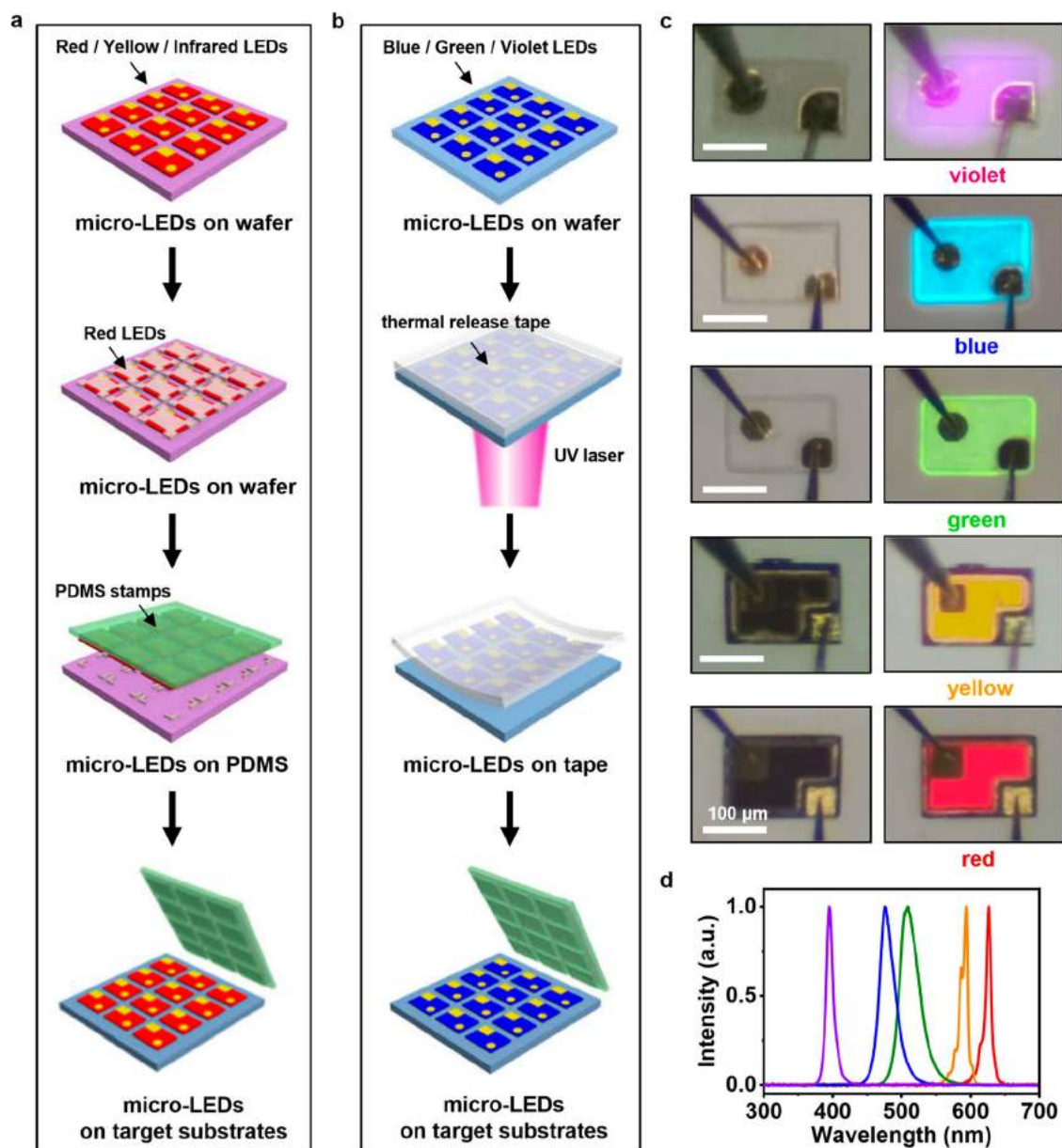
**Figure 1.** LED fabrication. a) Schematic illustration of the fabrication and transfer printing process for red, yellow and infrared LEDs. b) Schematic illustration of the fabrication and transfer printing process for blue, green and violet LEDs. c) Microscope images of various color micro-LEDs without (left) and with (right) electroluminescence. d) Electroluminescence spectra of various color micro-LEDs. The results for blue, green and red LEDs are reproduced with permission [33]. Copyright 2021, National Academy of Sciences. The results for violet and yellow LEDs are original.

to red, indicating that they maintain their light-emitting performance exceptionally well.

Nowadays, various transfer printing techniques have been developed for the mass production of micro-LEDs. The example mentioned above uses elastomer stamps to transfer devices via the Van der Waals force between the stamp and the device. This technique allows for transfering arrays of devices in a single cycle. In addition, the stamp can be reused over tens of thousands of

cycles [30]. Another modified approach employs electromagnetic force to pick up and transfer micro-LEDs. Alternatively, the electrostatic force method utilizes a specialized transfer head consisting of a pair of positively and negatively charged electrodes to pick up and print targeted devices [8]. These and other transfer printing techniques are actively exploited for the commercialization and industrialization of micro-LED based displays.

In addition to the lift-off and stamp transfer printing mentioned above, other approaches are also available for micro-LED fabrication. One method is wafer bonding, which enables the integration of III-V wafers and silicon wafers instead of bonding prefabricated devices, suitable for large-volume production [27, 28]. Another method is multilayer stacking based on Van der Waals force, which allows for the stacking of different 2D material layers to form a multilayer strucutre and offers high flexibility and low power consumption [36–38].

In recent times, researchers have successfully employed various materials of interest, such as printed circuit boards, flexible carriers, and biocompatible film, as new substrates for micro-LEDs [25, 33, 39–42]. As a result of these advanced manufacturing techniques, the range of potential applications for micro-LEDs has significantly expanded in display, optical treatment, and biosensing among other areas.

## 3. Micro-LED for display applications

Before 2000s, the cathode ray tube (CRT) was the pioneering technology for full-color display that gained widespread usage, but its bulky size, slow refresh rate, and radiation emissions were significant drawbacks. The advent of liquid crystal display (LCD) in the 2000s rendered CRT obsolete due to its portability and convenience [43, 44]. However, LCD has limitations including slow response time and inadequate color saturation, which hinder its development. Recently, organic light-emitting diode (OLED) technology has emerged as the display technology of choice in the market owing to its fast response time, high color contrast, and foldability [45, 46]. Despite its advantages, OLEDs face challenges such as a limited lifespan and screen burn-in phenomenon. Consequently, micro-LED based displays are emerging as the latest trend in display technology, owing to its high brightness, small form factor, and extended lifespan [6, 8, 26]. While monochrome micro-LED displays were invented in the 2000s [13], full-color micro-LED technology has advanced considerably, with the main methods for achieving it including combining horizontal or vertical RGB monochrome micro-LEDs, quantum dot conversion, and nanowire micro-LEDs [7].

To achieve full-color micro-LED displays directly, the most common method is to combine RGB monochrome micro-LEDs through flip-chip bonding and horizontal arrangement on specialized display panels. Various types of full-color micro-LED displays have been reported [47–50], such as a full-color LED projector on silicon micro-displays, which combines AlGaInP and GaN micro-LED arrays with active-matrix (AM) panels on silicon substrates using flip-chip bonding [50]. To further simplify the layout and wiring of micro-LEDs and improve manufacturing efficiency, a new approach called PixelEngine All-in-One has been developed [51]. This approach involves using a printable pixel-driver microIC with 3D integrated RGB micro-LEDs, which are combined with an intermediate substrate (Figure 2a). A 70 PPI (Pixels Per Inch) 5.1" full-color transparent micro-LED display has been successfully demonstrated using this approach (Figure 2b). The PixelEngine All-in-One method enhances transfer printing efficiency, reduces manufacturing cycles, and simplifies control circuit design. These features promote the industrialization and commercialization of full-color micro-LED displays.

To achieve high-resolution full-color micro-LED displays, an alternative strategy is to vertically integrate RGB LEDs. The vertical stack approach enhances space utilization and mitigates the impact of LED size reduction. A tandem device scheme based on stacked RGB micro-LEDs for full-color displays has been proposed, which involves vertically assembling $125\,\mu m \times 60\,\mu m$ RGB thin-film micro-LEDs and a filter using epitaxial lift-off and transfer printing techniques (Figure 2c) [33]. The use of a long-pass filter interlayer improves the output light efficiency by transmitting high levels of red light from the InGaP-based micro-LED situated underneath it and reflecting blue and green light emitted by the GaN-based LEDs positioned above it. This method of vertically integrating RGB micro-LEDs with independent electrical contacts has been successfully applied to create a simple display (as shown in Figures 2d and e). Furthermore, researchers have attempted to reduce the size of stacked micro-LEDs to less than $20\,\mu m$, resulting in the development of a full-color display that utilizes vertically integrated RGB micro-LEDs [52]. The growth of minimal micro-LEDs on a two-dimensional (2D) materials-coated substrate has been achieved using a 2D layer transfer technique. This technique improves the array density and reduces the lateral dimensions of stacked micro-LEDs, making micro-LEDs more suitable for use in miniaturized electronic full-color displays, including those used in VR and AR.

In light of the challenges faced by current techniques for achieving full-color displays with micro-LEDs, quantum dots (QDs) color conversion is emerging as an alternative approach. It involves combining RGB QDs with single-color micro-LEDs to bypass the difficulties of integrating different LEDs and complex electrical connections. A pulsed spray coating method has been used to spray QDs layers and print them on UV LEDs to fabricate QDs-LEDs, which has been demonstrated to achieve RGB display arrays [53]. After that, an aerosol jet printing method that can obtain high-quality QDs
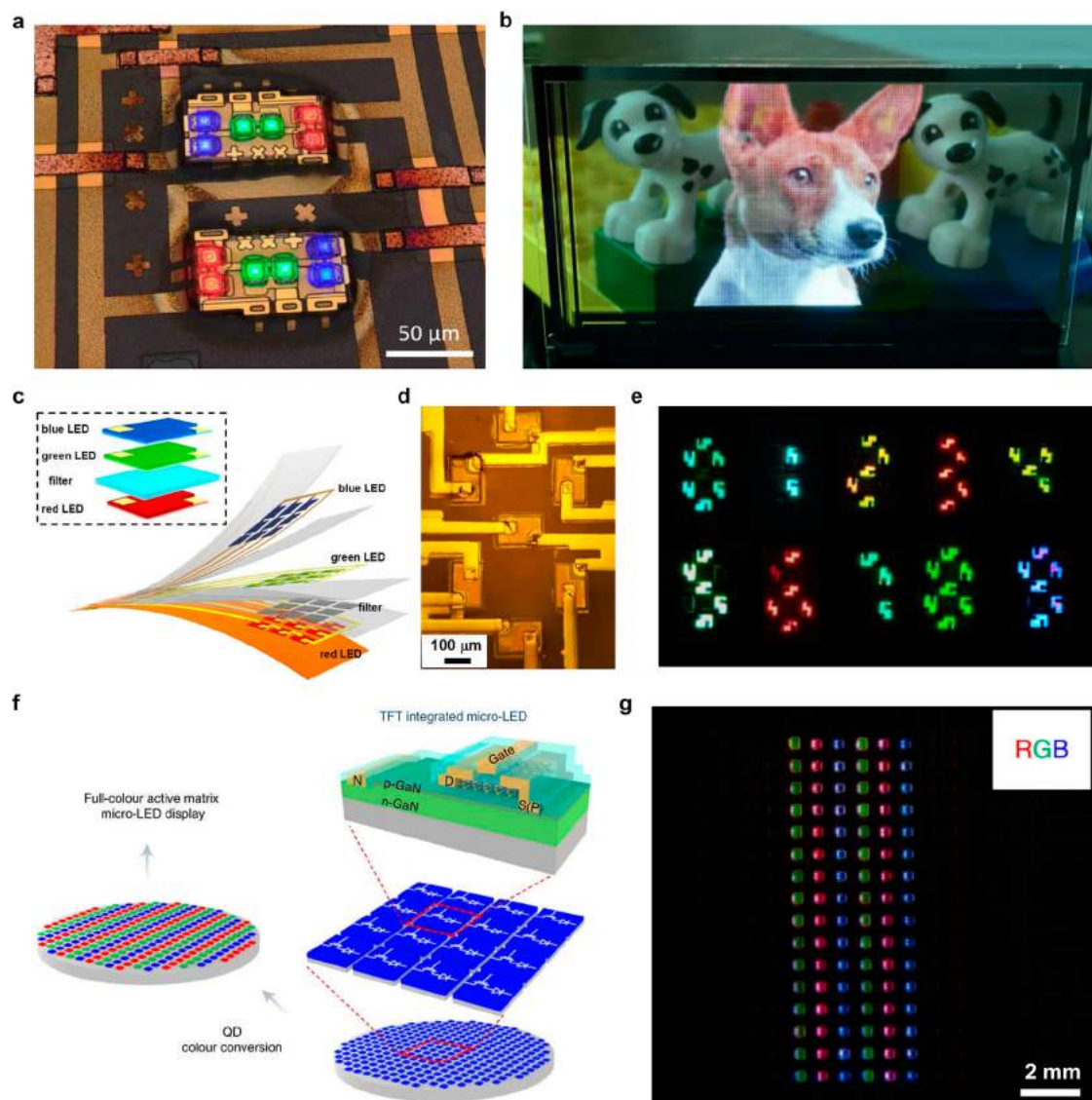
**Figure 2.** Micro-LEDs for display. a) Microscope image of energized PixelEngine All-in-Ones. b) Image of a 70 (pixels per inch) PPI5.1' full-color transparent micro-LED display. Reproduced with permission [51]. Copyright 2023, IEEE. c) Exploded schematic of stacked RGB microLED arrays. d) Microscope image of an array forming seven-segment display. e) Microscope image of colorful binary digits shown by seven-segment displays. Reproduced with permission [33]. Copyright 2021, National Academy of Sciences. f) Schematic of full-color micro-LEDs display with 2D semiconductor material TFTs and QDs. g) Microscope image of the full-color Micro-LEDs display with QDs color conversion. Reproduced with permission [38]. Copyright 2022, Nature Publishing Group.

using the atomizer and gas flow control is used to replace the pulsed spray coating method to print QDs on smaller LEDs to accomplish a full-color micro-LED display [54]. Another representative example is the integration of GaN-based micro-LEDs (with a lateral size of $10\,\mu m \times 10\,\mu m$) and $MoS_2$-based thin-film transistors (TFTs) for active switching. In this device configuration, CdSe/ZnS green and red quantum dots (QDs) are coated on blue micro-LEDs for effective color conversion. This integration has resulted in the development of a wafer-scale monolithic integrated full-color micro-LED display [38]. The $MoS_2$-based TFTs regulate the light intensity

of the micro-LEDs located underneath by controlling the gate voltage $V_{GS}$, and the CdSe/ZnS green and red colloidal QDs were patterned onto the micro-LEDs for effective color conversion (Figure 2f). The resulting display with 508 PPI yielded excellent characteristics as a color converter with high external quantum efficiency for both green and red QDs (Figure 2g). These techniques demonstrate great potential for developing a wafer-scale monolithic integrated full-color micro-LED display. In addition, by further reducing the size of micro-LEDs to the nanoscale, the bandgap energy of III–V materials can be altered due to quantum confinement effects.

**Table 1.** Comparison of representative full-color micro-LED display technologies.

| Method | Size (μm$^2$) | PPI | Thickness (μm) |
|---|---|---|---|
| Horizontal RGB micro-LEDs [51] | 120 | 70 | $\sim 5$ |
| Vertical stacked RGB micro-LEDs [52] | 16 | 5100 | $\sim 9$ |
| Quantum dot conversion [38] | 100 | 508 | $\sim 5$ |
| Nanowire micro-LEDs [57] | 0.24 | 1270 | $\sim 0.7$ |

This lead to a tunable wavelength of the emitted light over a wide range [55–57]. Nanoscale LEDs, such as nanowire LEDs, can be fabricated through e-beam lithography and dry etching techniques. InGaN/GaN based multiple-quantum-shell nanowire LEDs have been developed, enabling multi-color emission with a nanowire spacing of 1.2 μm [58]. Furthermore, InP/ZnO heterojunction nanowire LEDs have also demonstrated diverse wavelength peaks [59]. Nanowire LEDs offer advantages such as higher resolution, lower power consumption, and improved color accuracy.

To summarize, micro-LEDs have shown great potential in revolutionizing the display industry owing to their high efficiency, fast response time, and ease of combination with color converters [6, 8]. In Table 1, we summarize some representative works to realize full-color micro-LED displays with different strategies, including horizontally positioned RGB pixels, vertically stacked RGB pixels, emitters based on quantum dot conversion and nanowire based micro-LEDs. Although achieving full-color display with micro-LEDs still presents some challenges, continuous advancements and contributions from researchers are expected to enable the widespread use of micro-LEDs in the near future.

## 4. Micro-LED for optogenetic stimulations

Micro-LEDs have shown great potential not only as promising candidates in display technology but also as efficient light sources for various biomedical applications. Due to their small size, high brightness, and low heat generation, they are ideal for use as light sources in medical procedures such as photodynamic therapy, photothermal therapy, and optogenetics-based therapies [60–62]. Optogenetics is a powerful technique for studying the function of neural circuits by genetically modifying specific neurons to express light-sensitive proteins called opsins [63]. When these opsins are exposed to specific wavelengths of light, neural activities could be selectively activated or inhibited in a noninvasive and reversible manner. To achieve optogenetic stimulation, an appropriate optical stimulator is essential, such as laser or LED sources with fibers or specially designed waveguides [64–66]. Micro-LED-based light stimulators have emerged as a compelling alternative for optogenetic researchers due to their small form factor, low heat generation, and ability to provide wireless stimulation [21, 64].

Various types of micro-LED-based devices have been developed to achieve wireless and portable optogenetic stimulation. These include stimulators that mount micro-LEDs on hard PCB plates or flexible substrates, devices that are battery-powered or charged through induction coils, implantable or non-implantable devices, and optrode or probe-type devices [21, 65, 67, 68]. For example, a pioneering probe-type stimulator is an injectable cellular-scale probe with micro-LEDs for optogenetic stimulation and sensing, which is integrated with several components, such as a platinum electrode, a silicon micro-PD, four blue GaN micro-LEDs, and a serpentine resistor for temperature sensing or heating on four thin epoxy layers (Figure 3a) [21]. To facilitate implantation, the flexible probe is bonded to the target tissue using an injection microneedle and a bio-absorbable adhesive (Figure 3b). The system, which includes the probe device and wireless module, is powered and controlled wirelessly through radio frequency (RF) scavenging. The probe system has been successfully used for optogenetic stimulation in mice (Figure 3c) and has a larger stimulation area compared to traditional fiber strategies, demonstrating its potential for applications in biology and medicine.

As a result, different types of micro-LED optogenetic stimulation probes have been developed based on this work, each with varying functions. One example is a wireless dual-color optoelectronic probe designed to achieve distinct stimulation of the same brain area [41]. The probe is composed of a blue InGaN-based micro-LED, a SiO$_2$/TiO$_2$ filter, and a red InGaP-based micro-LED mounted on a flexible polyimide substrate with Cu coating on the backside (Figure 3d). The blue and red micro-LEDs are stacked vertically in a single location to stimulate the same area, and they can be controlled independently (Figure 3e). This allows the probe to stimulate two different channelrhodopsins that are sensitive to different wavelengths through the blue and red micro-LEDs, respectively (Figure 3f). This design enables the probe to achieve both cell depolarization and hyperpolarization, depending on the channelrhodopsin targeted by related light stimulation. In addition, the transfer printing technique enables the assembly of two micro-LEDs on the same probe, which can elicit distinct freezing and flight behaviors in mice by illuminating brain regions at different brain depths (Figure 3g) [69].

In addition to using single micro-LEDs as implantable light sources for multi-channel optogenetic stimulation,
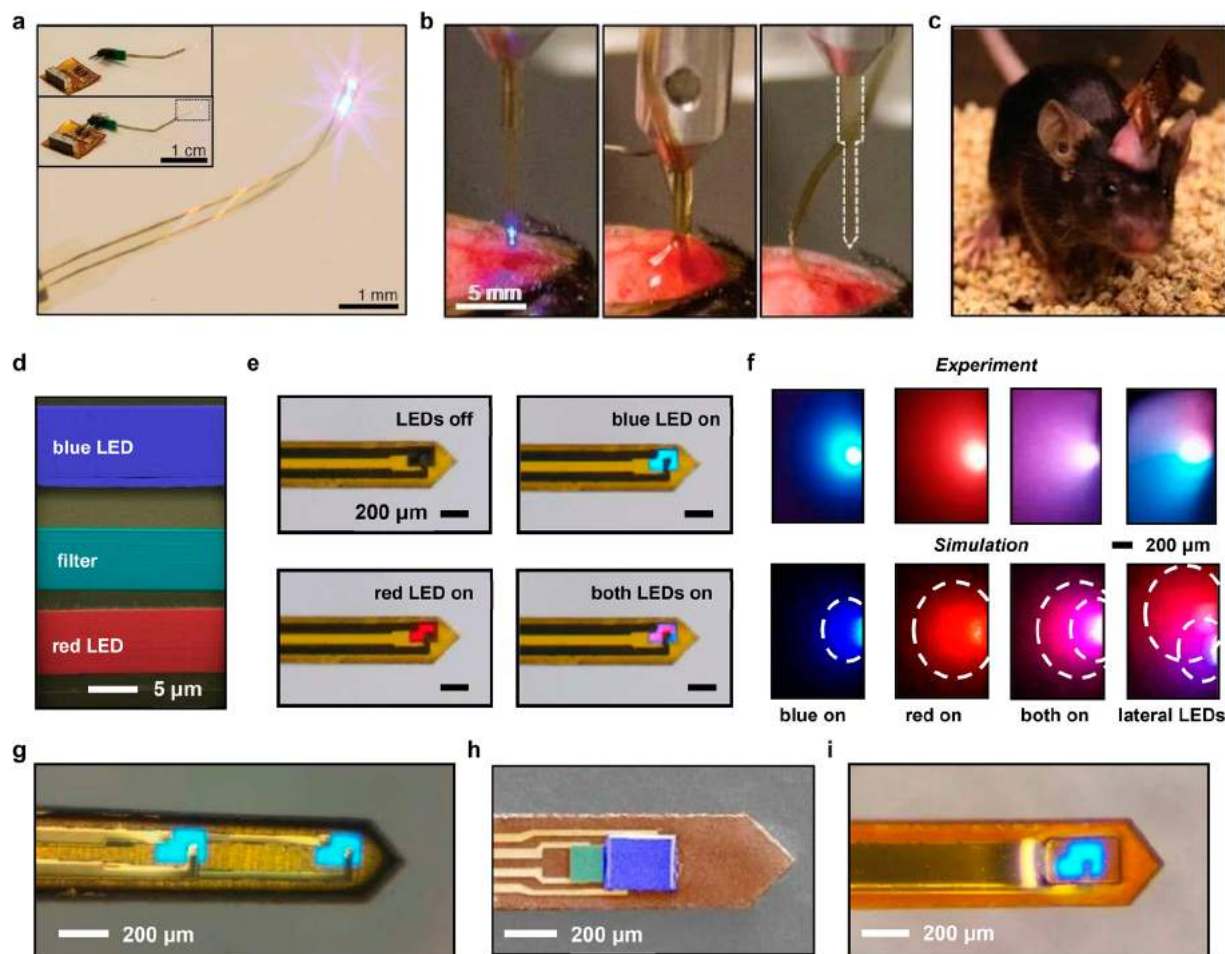
**Figure 3.** Micro-LEDs for optogenetic stimulations. a) Photograph of a wireless micro-LEDs optogenetic probe type stimulator and the device unconnected (top) and connected (bottom) to the power system. b) Photographs of the injection and release process of the microneedle. c) Photograph of the freely moving mouse with the wireless stimulator. Reproduced with permission [21]. Copyright 2013, AAAS. d) SEM image of a wireless dual-color optogenetic probe. e) Optical image of four different control models of the probe showing the independent control of different color micro-LEDs. f) Experimental photographs and simulated results of blue and red light propagation from a probe implanted in the brain. Reproduced with permission [41]. Copyright 2022, Nature Publishing Group. g) Photograph of a dual-channel optogenetic stimulation probe. Reproduced with permission [69]. Copyright 2022, Cell Press. h) Photograph of an optogenetic probe composed of micro-LED and micro-PD. Reproduced with permission [70]. Copyright 2018, National Academy of Sciences. i) Photograph of an optoelectrochemical probe composed of micro-LED and dopamine detector. Reproduced with permission [40]. Copyright 2018, National Academy of Sciences. Copyright 2022, Nature Publishing Group.

multifunctional probes can be achieved by incorporating these micro-LEDs with other devices to detect biosignals. For instance, a wireless optoelectronic probe is developed that combines a micro-LED, a GaAs micro-photodetector (micro-PD), and a filter to enable both stimulation and monitoring of neuronal activity (Figure 3h) [70]. The micro-PD in the probe is capable of detecting fluorescence-related neuronal activities, while the filter absorbs the redundant excitation light from micro-LED and allows the transmission of fluorescence to achieve high-quality optical signals. This multifunctional probe is successfully applied to wirelessly record transient calcium activity in the

basolateral amygdala (BLA) of mice, demonstrating its potential for use in neuroscience research. Another comparable probe integrates micro-LEDs and a chemical sensor to enable both optogenetic stimulation and dopamine detection [40]. The probe is comprised of four vertically integrated layers: a flexible substrate, a blue InGaN micro-LED for optogenetics stimulation, an undoped thin-film diamond layer for electrical isolation and heat dissipation, and a PEDOT:PSS film serving as an electrochemical sensor for dopamine detection (Figure 3i). By implanting the integrated probe into freely moving animals, it has been demonstrated that the probe is capable of achieving remote optogenetic

stimulation and dopamine signal monitoring in the same region.

Overall, implantable probes based on micro-LEDs have gained popularity as one of the optimal light delivery options for optogenetic stimulators owing to their small size, low power dissipation, and compatibility with other optical and electrical devices. However, controlling stimulation across the entire brain still remains a challenge, and researchers are currently working on addressing these issues. One approach involves the use of a wireless optogenetic stimulation probe that integrates five GaN micro-LEDs into a 2 mm tip to stimulate the deeper areas of the brain, although the width of stimulation is still limited [71]. An alternative solution is to use thin-film flexible GaN-based micro-LED arrays that can stimulate the brain's surface and control the horizontal spatial distribution. However, it is not suitable for stimulating deep brain areas [72]. To achieve more comprehensive, three-dimensional, and versatile optogenetic stimulation, further research is needed to develop advanced optogenetic stimulators.

## 5. Micro-LED for biosensing

While the micro-LEDs can be reliably used as implantable light sources for optical stimulation, they are also effective wireless sensors in detecting environmental factors. The electrical and optical properties of micro-LEDs, including their current, voltage, resistance, central emission wavelength, and light intensity, can be affected by external factors such as pressure, temperature, and contact resistance. Consequently, it is particularly advantageous to use micro-LEDs to detect environmental factors that impact their properties. Epitaxial lift-off and transfer printing technology enable the integration of micro-LEDs with biocompatible and flexible substrates or other functional devices, making them ideal for biosensing applications due to their small size, excellent luminous properties, and low power consumption.

Micro-LEDs exhibit high sensitivity to external environmental factors, thereby promoting the development of micro-LED sensors. For example, the photon-recycling effect of micro-LEDs has been utilized for biophysical and biochemical sensing, with the capabilities of light energy harvesting (photovoltaic effects), electrical signal amplification (the characteristics of diodes), and optical signal transmission (photoluminescence) [73, 74]. By exploiting the super-linear relationship between the emission intensity of micro-LEDs and external resistance, the galvanic skin response (GSR) in response to external stimuli has been wirelessly recorded with a camera mounted on the fluorescence microscope (Figures

4a, b, and c) [25]. In addition to GSR, micro-LEDs connected to other resistance-dependent devices, such as thermistors and piezoresistors can be used to measure changes in temperature (Figure 4d) or pressure (Figure 4e). Different from the photoluminescent properties of the micro-LED, the piezo-phototronic effect of nanowire LEDs has been exploited to develop a high-resolution pressure mapping sensor [23]. This sensor comprises a p-GaN thin-film/n-ZnO nanowire LED array integrated into a 200 μm PEF film and coated with a 300 μm ITO film, which serves as a transparent electrode. This subsequently facilitates the development of a high-resolution pressure mapping sensor (Figure 4f). The piezo-phototronic effect generates polarization charges at the interface of the p-n junction under applied pressure which influences the energy bandgap and exhibits a linear relationship with the enhancement of the light intensity (Figure 4g). A 'BINN' shaped sapphire stamp is placed on top of the device to verify the sensor's effectiveness. When external pressure is applied to the stamp, the LED intensities under the sapphire stamp increase, while the rest of the parts remain dark (Figure 4h). The experimental results confirm the capabilities of the sensor in detecting pressure and suggest potential applications in touch panels, smart skin, and other areas.

Integrating micro-LEDs with various sensors has proven to be a promising strategy in the area of biosensing. Unlike strategies based on the photon recycling effect, micro-LEDs have been used to measure temperature and pressure by combining them with thermistors, photodetectors or piezoresistors [25, 75]. Another example is the epidermal electronic system, which integrates multiple sensors, micro-LEDs, wireless power circuits, and RF communication circuits on a thin and flexible polyester substrate. This system allows for the detection of electrophysiological signals and optical characterization of skin or fluids [22]. These integrated micro-LEDs not only facilitate body surface sensors but can also enable *in vivo* biosensing. To further facilitate integration and *in vivo* application, microscopic sensors that utilize wireless optical integrated circuits containing micro-LEDs and other optoelectronics devices have been reported [24]. This miniaturized circuit, measuring 175 μm × 75 μm × 8 μm, is capable of wireless, in vivo monitoring of ion concentration in solutions, which comprises a micro-LED for optical signal output, silicon photovoltaics for power supply, a MOSFET, and input electrodes for sensing environmental signals (Figure 4i). The voltage drop of the circuit is proportional to the conductivity between two electrodes in the solution, allowing for the measurement of ion concentration. As the remaining voltage determines the output
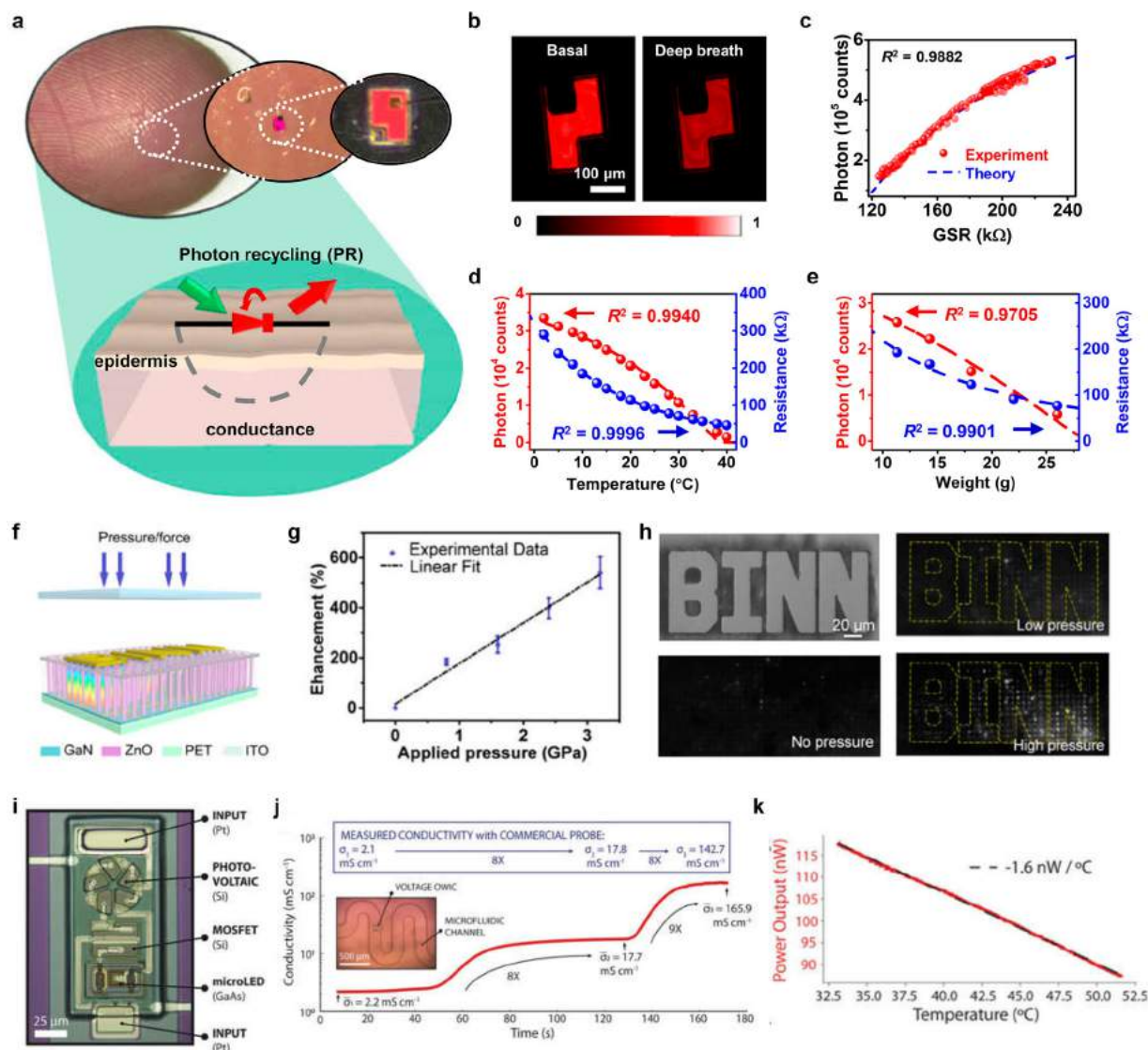
**Figure 4.** Micro-LEDs for biosensing. a) Photographs and schematic of a red micro-LED sensor on human skin based on photo recycling (PL) effect. b) Microscope images of PL emission intensities of micro-LED which are different under basal (left) and deep breathe (right) condition. c) Experiment and theory results of PL intensity of micro-LED changed with GSR. d) Experiment (dots) and theory (lines) results of PL intensity and resistance changed with temperature. e) Experiment (dots) and theory (lines) results of PL intensity and resistance changed with pressure. Reproduced with permission [25]. Copyright 2021, Springer Link. f) Schematic illustration of a pressure mapping using the piezo-phototronic effect of nanowire LEDs. g) A linear fit between enhancement factor of the LED emission intensity and applied pressure value of the strain sensor. h) Microscope images of a 'BINN' shaped sapphire stamp mounted on the top of the pressure mapping. Emitting intensities of LEDs under the sapphire are enhanced with the increase of pressure. Reproduced with permission [23]. Copyright 2019, Elsevier. i) Microscope image of a microscopic sensor using optical wireless integrated circuits (OWIC). j) OWIC and commercial probe measure results of local solution conductivity in the microfluidic channel. The insert picture is the microscope image of the OWICs in the channel. k) The characteristic of optical power output of the OWIC as a function of temperature. Reproduced with permission [24]. Copyright 2021, National Academy of Sciences.

light intensities of the micro-LED in the circuit, these optical signals can also reflect the solution conductivity, especially in a sealed microfluidic channel. The measured results are comparable to those obtained with a commercial product (Figure 4j). To clarify, the efficiency of the micro-LEDs and silicon photovoltaic cells can be affected by changes in temperature, which in

turn can affect the output light intensities and voltage drop of the circuit. By monitoring these changes, the circuit can also be used to measure temperature (Figure 4k).

Overall, micro-LEDs have proven to be promising biosensing tools due to their sensitivity to changes in emission intensity, easy arraying capabilities, and

compatibility with wireless and implantable designs. The integration of micro-LEDs with specialized substrates, optoelectronic devices, and biochemical sensors using advanced epitaxial lift-off and transfer printing technologies has expanded their potential applications in sensing. These advantages demonstrate the potential of micro-LED-based biosensors as a powerful tool in the field of biosensing.

## 6. Summary and outlook

This paper provides a comprehensive overview of the developmental history, advanced manufacturing techniques, and applications of III-V micro-LEDs. The unique advantages of thin-film micro-LEDs, including small size, high light intensity, high conversion efficiency, and low heat generation, make them ideal for a range of applications, including high-resolution display technology, implantable light sources for optogenetic stimulation, and wireless biosensing. The fabrication process of thin-film micro-LEDs is discussed in detail, with a particular emphasis on epitaxial lift-off, and transfer printing techniques that allow for integration into new substrates or other devices. Various methods have been developed to realize full-color micro-LED displays, such as assembling horizontal or vertical RGB monochrome micro-LEDs, quantum dot conversion, and nanowire devices. In addition to displays, micro-LEDs have also shown great potential in biomedical applications. Integrating micro-LEDs onto flexible substrates as implantable light source probes can efficiently deliver light to the brain to perform optogenetics stimulation and detect the neuron activities-related signals with other sensors. Moreover, micro-LEDs possess advantageous features for biosensing, such as sensitivity to changes in emission intensity, easy arraying due to their small size, and compatibility with wireless and implantable designs. These characteristics make micro-LEDs-based devices a new class of wireless sensors capable of detecting environmental factors such as pressure, temperature, and resistance.

In addition to their applications in the fields of displays and biomedical sensing, micro-LED technology is also being utilized in various other sectors. For instance, a recent study has reported the use of an InGaN micro-LED array for underwater wireless optical communication and charging [76]. A new trend in micro-LED research is to combine it with deep learning to achieve complex and precise data processing and analysis [77–79]. A recent study has explored a novel direction in micro-LED research by combining UV GaN micro-LEDs with semiconductor metal oxide-type gas sensors to create a convolutional neural network (CNN)

for use as an electronic nose system [79]. The system described above is designed to detect changes in gas resistance and accurately predict different target gases in real-time, demonstrating the potential of micro-LED technology in combination with deep learning and artificial intelligence. Another attractive direction is combining micro-LED devices with consumer electronic products such as mobile phones or computers [80, 81]. A fluorescence sensor is developed that utilizes a blue GaN micro-LED 1D array to excite quantum dot fluorescent targets, with the smartphone detecting fluorescence through a glass waveguide [80]. These additional applications of micro-LED technology demonstrate its versatility and potential for further advancements in various fields beyond displays and biomedical applications.

To summarize, this review showcases the potential impact of III-V micro-LEDs in various fields, highlighting their advanced manufacturing techniques and diverse applications. Further research and development in this area could lead to tremendous advancements in people's daily lives, particularly in the areas of displays, interactions, healthcare, and treatment. Therefore, the future of III-V micro-LEDs has the potential to revolutionize our lifestyles.

## Disclosure statement

No potential conflict of interest was reported by the author(s).

## Funding

## Notes on contributors

**Junyu Chen** received his B.Eng. degree from the Department of Electronic Engineering, Tsinghua University in Beijing, China, in 2022. He is currently pursuing his Ph.D. degree at the Department of Electronic Engineering, Tsinghua University.

**He Ding** received his Ph.D. degree from Ecole Centrale de Lyon, France, in 2016 and subsequently engaged in postdoctoral studies at Tsinghua University from 2016 to 2018. He is currently an Assistant Professor with the School of Optics and Photonics, Beijing Institute of Technology in Beijing, China.
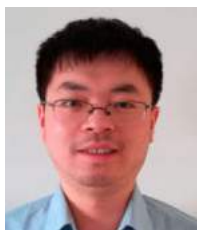
***Xing Sheng*** obtained his PhD degree from Massachusetts Institute of Technology in 2012, and his B.Eng degree from Tsinghua University in China in 2007. He is currently an Associate Professor in the Department of Electronic Engineering, and an Affiliated Researcher in the IDG/McGovern Institute for Brain Research, both at Tsinghua University.

## ORCID

*Junyu Chen* http://orcid.org/0000-0002-3501-8302
*He Ding* http://orcid.org/0000-0002-0884-3112
*Xing Sheng* http://orcid.org/0000-0002-8744-1700

## References

[1] H.J. Round, Electr World. **19**, 309 (1907).
[2] R.N. Hall, G.E. Fenner, J.D. Kingsley, T.J. Soltys, and R.O. Carlson, Phys. Rev. Lett. **9** (9), 366 (1962).
[3] M.I. Nathan, W.P. Dumke, G. Burns, F.H. Dill Jr, and G. Lasher, Appl. Phys. Lett. **1** (3), 62 (1962).
[4] R.A. Logan, H.G. White, and W. Wiegmann, Appl. Phys. Lett. **13** (4), 139 (1968).
[5] S. Nakamura, M. Senoh, and T. Mukai, Appl. Phys. Lett. **62** (19), 2390 (1993).
[6] Y. Huang, E.L. Hsiang, M.Y. Deng, and S.T. Wu, Light Sci. Appl. **9** (1), 105 (2020).
[7] J.Y. Lin, and H.X. Jiang, Appl. Phys. Lett. **116** (10), 100502 (2020).
[8] T. Wu, C.W. Sher, Y. Lin, C.F. Lee, S. Liang, Y. Lu, S.W. Huang Chen, W. Guo, H.C. Kuo, and Z. Chen, Appl. Sci. **8** (9), 1557 (2018).
[9] T. Ni, G.S. Schmidt, O.G. Staadt, M.A. Livingston, R. Ball, and R. May, presented at the IEEE Virtual Reality Conference (VR 2006), 2006 (unpublished).
[10] E.L. Hsiang, Z. Yang, Q. Yang, P.C. Lai, C.L. Lin, and S.T. Wu, Adv. Opt. Photonics **14** (4), 783 (2022).
[11] C.C. Lin, Y.H. Fang, M.J. Kao, P.K. Huang, F.P. Chang, L.C. Yang, and C.I. Wu, presented at the SID Symposium Digest of Technical Papers, 2018 (unpublished).
[12] S.X. Jin, J. Li, J.Z. Li, J.Y. Lin, and H.X. Jiang, Appl. Phys. Lett. **76** (5), 631 (2000).
[13] H.X. Jiang, S.X. Jin, J. Li, J. Shakya, and J.Y. Lin, Appl. Phys. Lett. **78** (9), 1303 (2001).
[14] Z. Su, M. Zhanghu, and Z. Liu, presented at the SID Symposium Digest of Technical Papers, 2021 (unpublished).
[15] F. Templier, presented at the SID Symposium Digest of Technical Papers, 2021 (unpublished).
[16] R. Karthika, and S. Balakrishnan, SSRG Int. J. Electron. Commun. Eng. (SSRG-IJECE) **2** (3), 32 (2015).
[17] H. Haas, L. Yin, Y. Wang, and C. Chen, J. Lightwave Technol. **34** (6), 1533 (2016).
[18] N. Bamiedakis, X. Li, J.J. McKendry, E. Xie, R. Ferreira, E. Gu, M.D. Dawson, R.V. Penty, and I.H. White, presented at the 2015 17th international conference on transparent optical networks (ICTON), 2015 (unpublished).
[19] V. Poher, N. Grossman, G.T. Kennedy, K. Nikolic, H.X. Zhang, Z. Gong, E.M. Drakakis, E. Gu, M.D. Dawson, P.M.W. French, and P. Degenaar, J. Phys. D: Appl. Phys. **41** (9), 094014 (2008).
[20] N. Grossman, V. Poher, M.S. Grubb, G.T. Kennedy, K. Nikolic, B. McGovern, R.B. Palmini, Z. Gong, E.M. Drakakis, M.A. Neil, and M.D. Dawson, J. Neural Eng. **7** (1), 016004 (2010).
[21] T.I. Kim, J.G. McCall, Y.H. Jung, X. Huang, E.R. Siuda, Y. Li, J. Song, Y.M. Song, H.A. Pao, R.H. Kim, and C. Lu, Science **340** (6129), 211 (2013).
[22] D.H. Kim, N. Lu, R. Ma, Y.S. Kim, R.H. Kim, S. Wang, J. Wu, S.M. Won, H. Tao, A. Islam, and K.J. Yu, Science **333** (6044), 838 (2011).
[23] Y. Peng, M. Que, H.E. Lee, R. Bao, X. Wang, J. Lu, Z. Yuan, X. Li, J. Tao, J. Sun, and J. Zhai, Nano Energy **58**, 633 (2019).
[24] A.J. Cortese, C.L. Smart, T. Wang, M.F. Reynolds, S.L. Norris, Y. Ji, S. Lee, A. Mok, C. Wu, F. Xia, and N.I. Ellis, Proc. Nat. Acad. Sci. **117** (17), 9173 (2020).
[25] H. Ding, G. Lv, Z. Shi, D. Cheng, Y. Xie, Y. Huang, L. Yin, J. Yang, Y. Wang, and X. Sheng, Nano Res. **14** (9), 3208 (2021).
[26] V.W. Lee, N. Twu, and I. Kymissis, Inf. Disp. **32** (6), 16 (2016).
[27] B. Corbett, R. Loi, W. Zhou, D. Liu, and Z. Ma, Prog. Quantum Electron. **52**, 1 (2017).
[28] L. Zhang, F. Ou, W.C. Chong, Y. Chen, and Q. Li, J. Soc. Inf. Disp. **26** (3), 137 (2018).
[29] S.I. Park, Y. Xiong, R.H. Kim, P. Elvikis, M. Meitl, D.H. Kim, J. Wu, J. Yoon, C.J. Yu, Z. Liu, and Y. Huang, Science **325** (5943), 977 (2009).
[30] R.S. Cok, M. Meitl, R. Rotzoll, G. Melnik, A. Fecioru, A.J. Trindade, B. Raymond, S. Bonafede, D. Gomez, T. Moore, and C. Prevatte, J. Soc. Inf. Disp. **25** (10), 589 (2017).
[31] D.M. Geum, S.K. Kim, C.M. Kang, S.H. Moon, J. Kyhm, J. Han, D.S. Lee, and S. Kim, Nanoscale **11** (48), 23139 (2019).
[32] C.M. Kang, D.J. Kong, J.P. Shim, S. Kim, S.B. Choi, J.Y. Lee, J.H. Min, D.J. Seo, S.Y. Choi, and D.S. Lee, Opt. Express **25** (3), 2489 (2017).
[33] L. Li, G. Tang, Z. Shi, H. Ding, C. Liu, D. Cheng, Q. Zhang, L. Yin, Z. Yao, L. Duan, and D. Zhang, Proc. Nat. Acad. Sci. **118** (18), e2023436118 (2021).
[34] H.S. Kim, E. Brueckner, J. Song, Y. Li, S. Kim, C. Lu, J. Sulkin, K. Choquette, Y. Huang, R.G. Nuzzo, and J.A. Rogers, Proc. Nat. Acad. Sci. **108** (25), 10072 (2011).
[35] C. Youtsey, R. McCarthy, R. Reddy, K. Forghani, A. Xie, E. Beam, J. Wang, P. Fay, T. Ciarkowski, E. Carlson, and L. Guido, Phys. Status Solidi B **254** (8), 1600774 (2017).
[36] Q. He, Z. Zeng, Z. Yin, H. Li, S. Wu, X. Huang, and H. Zhang, Small **8** (19), 2994 (2012).
[37] Z. Lin, Y. Liu, U. Halim, M. Ding, Y. Liu, Y. Wang, C. Jia, P. Chen, X. Duan, C. Wang, and F. Song, Nature **562** (7726), 254 (2018).
[38] S. Hwangbo, L. Hu, A.T. Hoang, J.Y. Choi, and J.H. Ahn, Nat. Nanotechnol. **17** (5), 500 (2022).
[39] Y. Zhao, C. Liu, Z. Liu, W. Luo, L. Li, X. Cai, D. Liang, Y. Su, H. Ding, Q. Wang, and L. Yin, IEEE Trans Electron Devices **66** (1), 785 (2019).
[40] C. Liu, Y. Zhao, X. Cai, Y. Xie, T. Wang, D. Cheng, L. Li, R. Li, Y. Deng, H. Ding, and G. Lv, Microsys Nanoeng **6** (1), 64 (2020).

[41] B. Li, A. Deng, K. Li, Y. Hu, Z. Li, Y. Shi, Q. Xiong, Z. Liu, Q. Guo, L. Zou, and H. Zhang, Nature Commun **13** (1), 1 (2022).

[42] Y. Xie, H. Wang, D. Cheng, H. Ding, D. Kong, L. Li, L. Yin, G. Zhao, L. Liu, G. Zou, and J. Wei, J. Phys. D: Appl. Phys. **54** (38), 384004 (2021).

[43] J.P. Boeuf, J. Phys. D: Appl. Phys. **36** (6), R53 (2003).

[44] N. Chang, I. Choi, and H. Shim, IEEE Trans. Very Large Scale Integr. (VLSI) Syst. **12** (8), 837 (2004).

[45] H.W. Chen, J.H. Lee, B.Y. Lin, S. Chen, and S.T. Wu, Light Sci. Appl. **7** (3), 17168 (2018).

[46] B. Geffroy, P.L. Roy, and C. Prat, Polym. Int. **55** (6), 572 (2006).

[47] D. Peng, K. Zhang, V.S.D. Chao, W. Mo, K.M. Lau, and Z. Liu, J. Disp. Technol. **12** (7), 742 (2016).

[48] C.A. Bower, M.A. Meitl, B. Raymond, E. Radauscher, R. Cok, S. Bonafede, D. Gomez, T. Moore, C. Prevatte, B. Fisher, and R. Rotzoll, Photonics Res. **5** (2), A23 (2017).

[49] C.A. Bower, S. Bonafede, B. Raymond, A. Pearson, C. Prevatte, T. Weeks, E. Radauscher, E. Vick, C. Verreen, B. Krongard, and M.A. Meitl, presented at the 2020 IEEE 70th Electronic Components and Technology Conference (ECTC), 2020 (unpublished).

[50] Z.J. Liu, W.C. Chong, K.M. Wong, K.H. Tam, and K.M. Lau, IEEE Photonics Technol. Lett. **25** (23), 2267 (2013).

[51] C.A. Bower, B. Raymond, C. Verreen, C. Prevatte, S. Bonafede, A. Pearson, N. Rivers, B. Keller, T. Weeks, B. Trinh, and E. Vick, IEEE J. Sel. Top. Quantum Electron. **29** (3), 1 (2023).

[52] J. Shin, H. Kim, S. Sundaram, J. Jeong, B.I. Park, C.S. Chang, J. Choi, T. Kim, M. Saravanapavanantham, K. Lu, and S. Kim, Nature **614** (7946), 81 (2023).

[53] K.J. Chen, H.C. Chen, K.A. Tsai, C.C. Lin, H.H. Tsai, S.H. Chien, B.S. Cheng, Y.J. Hsu, M.H. Shih, C.H. Tsai, and H.H. Shih, Adv. Funct. Mater. **22** (24), 5138 (2012).

[54] H.V. Han, H.Y. Lin, C.C. Lin, W.C. Chong, J.R. Li, K.J. Chen, P. Yu, T.M. Chen, H.M. Chen, K.M. Lau, and H.C. Kuo, Opt. Express **23** (25), 32504 (2015).

[55] Y.H. Ra, R. Wang, S.Y. Woo, M. Djavid, S.M. Sadaf, J. Lee, G.A. Botton, and Z. Mi, Nano Lett. **16** (7), 4608 (2016).

[56] H.Q.T. Bui, R.T. Velpula, B. Jain, O.H. Aref, H.D. Nguyen, T.R. Lenka, and H.P.T. Nguyen, Micromachines **10** (8), 492 (2019).

[57] Y. Qian, Z. Yang, Y.H. Huang, K.H. Lin, and S.T. Wu, J Soc. Inf. Disp. **31** (5), 211 (2023).

[58] K. Ito, W. Lu, S. Katsuro, R. Okuda, N. Nakayama, N. Sone, K. Mizutani, M. Iwaya, T. Takeuchi, S. Kamiyama, and I. Akasaki, Nanoscale Adv. **4** (1), 102 (2021).

[59] N. Gagrani, K. Vora, L. Fu, C. Jagadish, and H.H. Tan, Nanoscale Horizons **7** (4), 446 (2022).

[60] J.F. Algorri, M. Ochoa, P. Roldán-Varona, L. Rodríguez-Cobo, and J.M. López-Higuera, Cancers **13** (14), 3484 (2021).

[61] M.A. Hadis, P.R. Cooper, M.R. Milward, P.C. Gorecki, E. Tarte, J. Churm, and W.M. Palin, J. Biophotonics **10** (11), 1514 (2017).

[62] I. Kirino, K. Fujita, K. Sakanoue, R. Sugita, K. Yamagishi, S. Takeoka, T. Fujie, S. Uemoto, and Y. Morimoto, Sci. Rep. **10** (1), 22017 (2020).

[63] F. Zhang, L.P. Wang, M. Brauner, J.F. Liewald, K. Kay, N. Watzke, P.G. Wood, E. Bamberg, G. Nagel, A. Gottschalk, and K. Deisseroth, Nature **446** (7136), 633 (2007).

[64] E.S. Edward, A.Z. Kouzani, and S.J. Tye, J. Neural Eng. **15** (2), 021002 (2018).

[65] C.T. Wentz, J.G. Bernstein, P. Monahan, A. Guerra, A. Rodriguez, and E.S. Boyden, J Neural Eng. **8** (4), 046021 (2011).

[66] M. Hashimoto, A. Hata, T. Miyata, and H. Hirase, Neurophotonics **1** (1), 011002 (2014).

[67] H.M. Lee, K.Y. Kwon, W. Li, and M. Ghovanloo, presented at the 2014 36th Annual International Conference of the IEEE Engineering in Medicine and Biology Society, 2014 (unpublished).

[68] S. Dufour, and Y. De Koninck, Neurophotonics **2** (3), 031205 (2015).

[69] X. Cai, L. Li, W. Liu, N. Du, Y. Zhao, Y. Han, C. Liu, Y. Yin, D. Sheng, and L. Yin, Iscience **25** (1), 103681 (2022).

[70] L. Lu, P. Gutruf, L. Xia, D.L. Bhatti, X. Wang, A. Vazquez-Guardado, X. Ning, X. Shen, T. Sang, R. Ma, and G. Pakeltis, Proc. Nat. Acad. Sci. **115** (7), E1374 (2018).

[71] H. Yasunaga, H. Takeuchi, K. Mizuguchi, A. Nishikawa, A. Loesing, M. Ishikawa, C. Kamiyoshihara, S. Setogawa, N. Ohkawa, and H. Sekiguchi, Opt. Express **30** (22), 40292 (2022).

[72] H. Sekiguchi, H. Matsuhira, R. Kanda, S. Tada, T. Kitade, M. Tsutsumi, A. Nishikawa, A. Loesing, I. Fukunaga, S. Setogawa, and N. Ohkawa, Appl. Phys. Express **15** (4), 046501 (2022).

[73] H. Ding, H. Hong, D. Cheng, Z. Shi, K. Liu, and X. Sheng, ACS Photonics **6** (1), 59 (2019).

[74] X. Sheng, M.H. Yun, C. Zhang, A.A.M. Al-Okaily, M. Masouraki, L. Shen, S. Wang, W.L. Wilson, J.Y. Kim, P. Ferreira, and X. Li, Adv. Energ. Mater. **5** (1), 1400919 (2015).

[75] H. Ding, G. Lv, X. Cai, J. Chen, Z. Cheng, Y. Peng, G. Tang, Z. Shi, Y. Xie, X. Fu, and L. Yin, Light Sci. Appl. **11** (1), 130 (2022).

[76] R. Lin, X. Liu, G. Zhou, Z. Qian, X. Cui, and P. Tian, Adv. Opt. Mater. **9** (12), 2002211 (2021).

[77] C.H. Huang, Y.T. Cheng, Y.C. Tsao, X. Liu, and H.C. Kuo, Photonics Res. **10** (2), 269 (2022).

[78] I. Kang, M. De Cea, J. Xue, Z. Li, G. Barbastathis, and R.J. Ram, Optica **9** (10), 1149 (2022).

[79] K. Lee, I. Cho, M. Kang, J. Jeong, M. Choi, K.Y. Woo, K.J. Yoon, Y.H. Cho, and I. Park, ACS Nano **17** (1), 539 (2023).

[80] N. Bruce, F. Farrell, E. Xie, M.G. Scullion, A.M. Haughey, E. Gu, M.D. Dawson, and N. Laurand, Biomed. Opt. Express **14** (3), 1107 (2023).

[81] A.D. Griffiths, J. Herrnsdorf, M.J. Strain, and M.D. Dawson, Opt. Express **27** (11), 15585 (2019).